SUMMARY OF WG3 ON INSTRUMENTATION, CONTROLS, AND BEAM LOSSES – ERL 2015

C. Gulliford, Cornell CLASSE, Ithaca, USA
T. Obina, KEK, Japan

Abstract

Here we summarize the work presented at the ERL 2015 concerning recent progress and issues with instrumentations, controls, and beam loss in the context of Energy Recovery Linacs.

INSTRUMENTATION, DIAGNOISTICS CONTROLS, AND BEAM LOSSES

The first talk described a non-destructive beam position monitoring method in two-beam section of KEK-cERL. The circumference about 90 m produces the time difference in pre- and post-accelerated beam. Typical macro-pulse length of 1 µs was observed as 300 ns non-overlapped signal and 700 ns overlapped signal, as seen in Figure 1. The non-overlapped part was used for beam position of two beams, as seen in Figure 2. By selecting the detection frequency, the overlapped part can be sensitive to the phase of two beams, thus the phase signal was used for path-length adjustment of the beam. The time-domain separation is also effective during the CW beam by introducing a short gap in the gun laser. This very simple method can be applied for ERL machines.
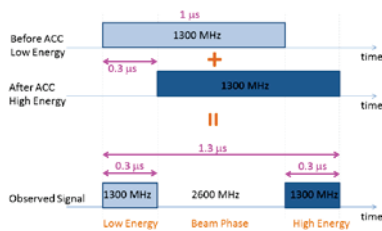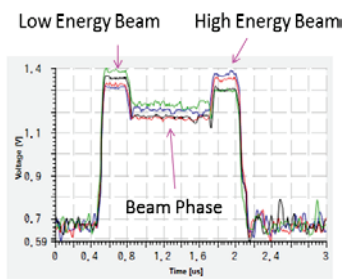

Figure 1: Principle of time separation.

Figure 2: Measurement results for two beams.

A detailed talk concerning diagnostics at ALICE was given. The ALICE facility at Daresbury Laboratory is an energy recovery based infra-red free electron laser of the oscillator type that has been operational since 2010. Fast diagnostics have been installed to perform combined measurements on pulse-by pulse FEL pulse energy and bunch-by-bunch electron bunch position and arrival time. These measurements have highlighted and quantified fast instabilities in the electron beam and consequently the FEL output, the first observation of which is shown in Figure 3. The material presented at ERL 2015 focussed on the instabilities, rather than technical details of the diagnostic hardware and processing techniques.

The ALICE beam energy is 25-30 MeV. The ALICE beam structure has 60 pC bunches at 16.25 MHz repetition frequency (i.e. bunches separated by 62 ns) in 100 µs bunch trains (there are around 1600 bunches in each train) produced at the machine repetition rate of 10 Hz.

A fast photo electromagnetic detector (PEM) was used to measure the intensity of the individual FEL pulses and had been used since shortly after lasing in 2010, and showed immediately a pronounced variation in FEL pulse intensity at around 100 kHz (see Figure 4 and Figure 5). There were, and still are, no applications of the ALICE FEL which are sensitive to this instability.
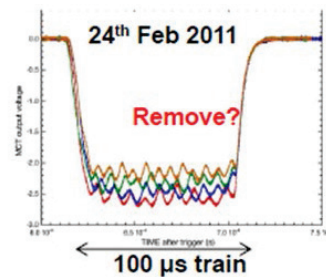

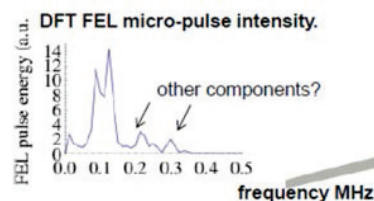Figure 3: First observation of instability in the FEL micropulse intensity.

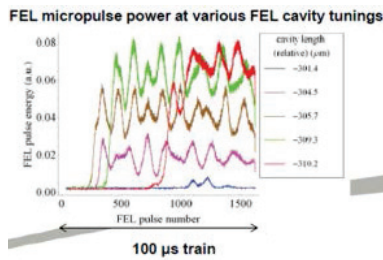Figure 4: Frequency components of the instability.

Figure 5: FEL micropulse intensity showing instability.

To investigate the source of this instability, fast BPM electronics (which had been originally developed for use on the EMMA non-scaling FFAG at Daresbury) were implemented at various locations in ALICE. They showed a pronounced instability at roughly 100 kHz in the bunch position, most clearly in the post-booster and post-linac lattice (see Figure 6). Pre-booster, the evidence for this instability was less clear. In addition, a ~300 kHz instability in the bunch charge was observed clearly at all locations; this sometimes appears in the FEL intensity at a much smaller amplitude than the 100 kHz signal.

To further investigate the root cause of the instabilities, the photoinjector laser was examined. A fast photodiode reveals a 300 kHz instability in the laser intensity, while the evidence for a ~100 kHz position instability of the laser beam is less convincing. It had in fact already been established in measurements in 2007 that the SSB spectra of the PI laser phase with respect to the RF reference showed an instability at 300 kHz.
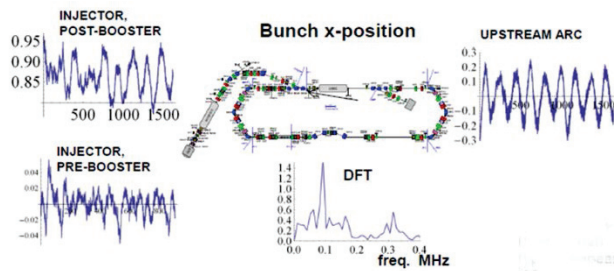

Figure 6: Position instability on fast BPMs.

In addition to the measurements described above, some measurements were performed synchronising fast PEM, BPM, and bunch time-of-arrival (TOA) measurements (using optical sampling of BPM signals) for individual machine shots. The motivation for this was as test bed for optical TOA diagnostics and as a potential source of extra information on the instabilities. The 100 kHz instability was also present in the TOA data and highly correlated with the other observables.

After presenting this material, several suggestions were made as to the root cause of the 100 kHZ instability. These included the DC gun power supply stability, stability of the

PI laser power supplies, and instabilities resulting from feedback loop from the low level RF. It was noted that the bunch position stability seemed to be more pronounced as the beam moved further downstream through the machine from the gun. These suggestions will be investigated further with the relevant technical groups at Daresbury.

Similarly, diagnostic work being done on the MESA project was discussed. The diagnostic test-beam-line for MESA shown in Figure 7 is built and ready for use. Investigations of the two transverse phase-spaces with quadrupole scan technique and the determination of the beam profile with a screen or with wires are possible. The beam-line gives the possibility of a cross check between quadrupole scan and slit mask measurements. The temporal distribution can be inspected with a deflecting cavity that transforms the longitudinal distribution into an transverse one and deflects the beam onto a circle which can be observed with a Ce:YAG screen and a CCD-camera, as shown in Figure 8. All this can be done with three different laser wavelengths (405, 520, 780nm) and for different laser spot sizes.
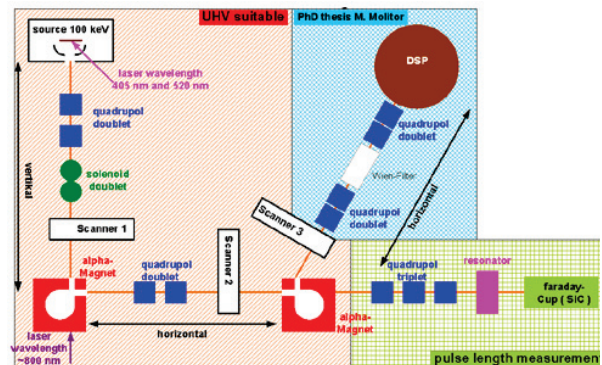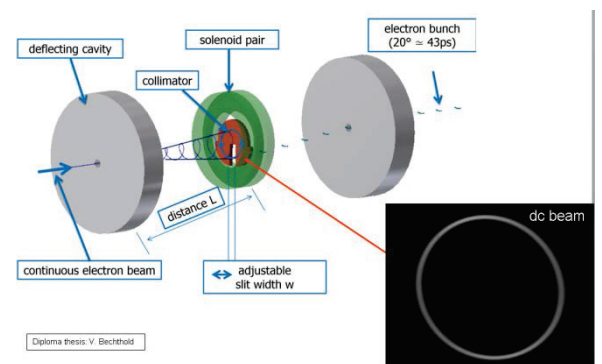

Figure 7: MESA diagnostic components.

Figure 8: MESA Deflecting Cavity and Collimator Set-up.

The first preliminary results of the emittance look promising to match the requirements of MESA stage 1. Further investigations of higher bunch charges etc. have to be done.

In the future it is planned to get more experience with the beam-line and the measurement techniques to characterize if the electron bunches from the source are suitable for MESA stage 1. Furthermore a closer look to helicity correlated halo effects is in preparation.

Additionally, a presentation was given on techniques to measure the beam current in the BNL ERL. This talk focused on the techniques of current measurements associated with machine protection against over exposure of instrumentation to beam charge at BNL's ERL. The machine layout was presented with an overview of installed instrumentation, followed by the beam operating parameters and the required current measurement ranges. The measurement technique & results from the Faraday Cup measurements made with beam were presented that revealed accurate measurements of the dark current produced by the SRF cavity as well as the current pulses produced by the photocathode. The method of charge measurement was described as an in-flange integrating current transformer (ICT) from Bergoz Electronics. The beam pulse length & repetition rate limitations were discussed, followed by results of measurements of beam charge that showed good agreement with the faraday cup. This was followed by a graphical depiction of the bunch, macrobunch & bunch train structures that were implemented to tailor to the requirements of the ICT.

The use of the ICT by the machine protection system was described showing the interface electronics. The MPS logic was described to have individual charge thresholds for each insertable instrument in the beam line. These limits are enabled by the insertion of the corresponding instrument. This mode is used with short macrobunches measured directly by the ICT. For recording current from longer macro bunches, a pulse counting scheme was proposed (but not yet implemented) where the laser pulses (at 9.38MHz) in the train are counted by a high-speed counter and multiplied by the measured charge per bunch in a short "pilot macro bunch". The result is processed by the control system with the bunch train structure to record an average current.

A DCCT, also made by Bergoz Electronics, was show to be installed in two places in the ERL for average current measurement when the bunch structure is composed of trains long enough to satisfy the bandwidth requirements of the DCCT. A technique of transitioning from a bunch structure compatible with the ICT to a bunch structure compatible with the DCCT was shown in a graphical depiction, where the average train current is 50μA in both cases. A differential current measurement scheme was mentioned as being under development. Discussions that followed the talk brought out the concern for shields to be installed in the vacuum to shield the ceramic breaks from the passing beam in an effort to avoid charge being deposited on the ceramic.

ION DIAGNOSTICS AND CLEARING METHODS

Experiments were recently performed to test the effectiveness of three ion-clearing strategies in the Cornell high intensity photoinjector: DC clearing electrodes, bunch gaps, and beam shaking. The photoinjector reaches a new regime of linac beam parameters where high CW beam currents make ion trapping unavoidable. Therefore ion mitigation strategies must be evaluated for this machine and other future ERLs.

Because high beam intensities present beam diagnostic challenges, several techniques were developed to directly measure the residual trapped ions rather than the beam. Two primary indicators of successful clearing are the amount of ion current removed by a DC clearing electrode, and the absence of bremsstrahlung radiation generated by beam-ion interactions. Measurements were taken for a 5 MeV electron beam and CW beam currents in the range of 1-20 mA.

Several theoretical models have been developed to explain the data. Using them, one can estimate the clearing electrode voltage required for maximum ion clearing (see Figure 9), the creation and clearing rates of the ions while employing bunch gaps, and the sinusoidal shaking frequency necessary for clearing via beam shaking. In all cases, a maximum ion clearing of at least 70 percent or higher was achieved, and almost full ion clearing was approached in certain cases.
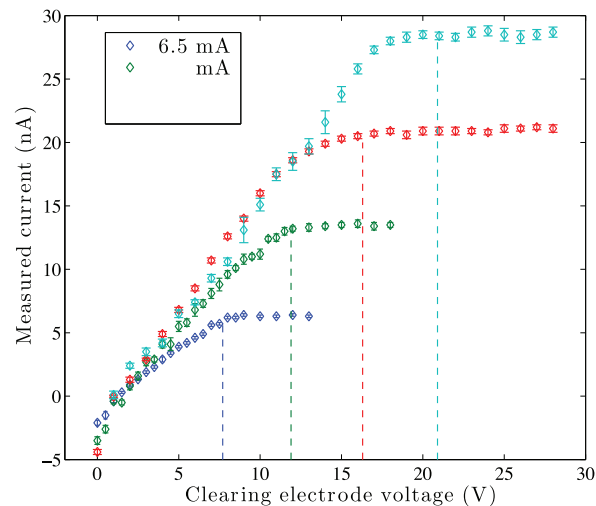

Figure 9: A picoammeter was used to measure the ion current striking the clearing electrode for different applied voltages. The vertical dotted lines mark the minimum voltage required for full ion clearing, as predicted using a simple theory.
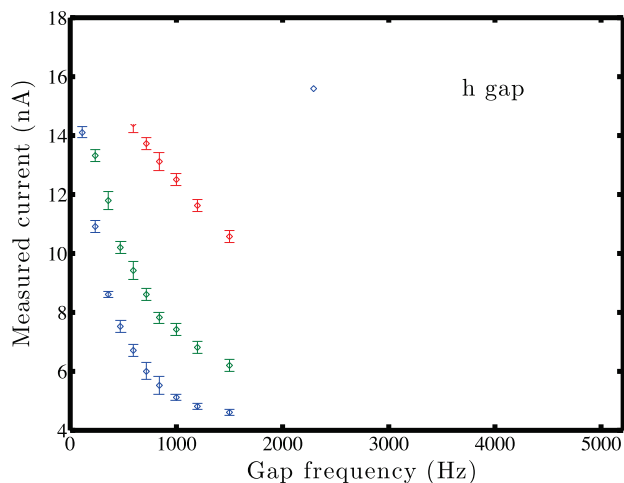
Figure 10: Increasing the frequency and duration of bunch gaps reduces the trapped ion density as shown by the residual ion current hitting a clearing electrode.

Of particular note is the finding that the total amount of clearing while employing bunch gaps does not depend strictly on the bunch gap duration and frequency. Instead, it depends only on the total time the beam is turned off, as is seen in Figure 10. This flexibility may allow it to be deployed in ERLs – a prospect previously thought too difficult to consider due to problems with beam loading.

A new diagnostic capable of surviving high intensity electron beams was discussed. It consists of a thin rotating wire that passes through the beam, and a downstream radiation detector. Together, they allow for a high current beam profile. The design was optimized to reduce the footprint of the device, while still allowing it to reach the large velocities needed to prevent it from absorbing too much heat load from the beam. It was installed in the Cornell injector, and tested at moderately high beam currents up to 20 mA, though at the relatively low energy and correspondingly large beam width inherent in injectors. Depending on the gain in the PMT radiation monitor, it could also be used at a much lower average current, and at these currents it was compared to a measurement on a viewscreen. Above a certain speed, which supressed the error from wire vibration, the two measurements were found to agree well, as in Figure 11.
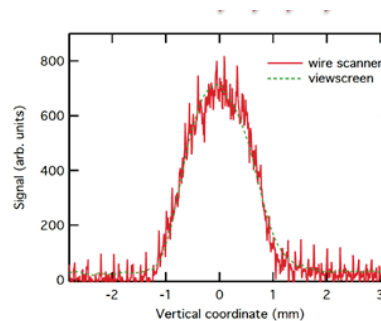

Figure 11: Comparison of the beam profile using the wire-scanner vs. viewscreen.

CONCLUSION

Progress continues to be made in the development of diagnostics suitable for the high intensity beams produced in Energy Recovery Linear accelerators. Instabilities were investigated at ALICE using various diagnostics including fast BPMs. The diagnostic beamline for MESA was discussed. The applicable range and performance benefits of competing designs for measuring beam current were covered, including ICTs and DCCTs. Finally, a report on effective methods of ion clearing as well as a new diagnostic for transverse beam profiles was given.

ACKNOWLEDGMENT